Published in final edited form as:
Endocr Relat Cancer. 2012 April ; 19(2): 111–122. doi:10.1530/ERC-10-0327.

Embryonic epithelial *Pten* deletion through *Nkx2.1-cre* leads to thyroid tumorigenesis in a strain-dependent manner

Caterina Tiozzo[1,2,3], **Soula Danopoulos**[1], **Maria Lavarreda-Pearce**[1], **Sheryl Baptista**[1], **Radka Varimezova**[1], **Denise Al Alam**[1], **David Warburton**[1], **Rehan Virender**[4], **Stijn De Langhe**[5], **Antonio Di Cristofano**[6], **Saverio Bellusci**[#1,7], and **Parviz Minoo**[#1,2]

[1]Developmental Biology Program, Saban Research Institute of Childrens Hospital Los Angeles, Los Angeles, California 90027, USA

[2]Department of Pediatrics, University of Southern California, Los Angeles, California 90027, USA

[3]Department of Pediatrics, Nassau University Medical Center, 201 Hempstead Turnpike, East Meadow, New York 11554, USA

[4]Department of Pediatrics, Los Angeles Biomedical Research Institute at Harbor-UCLA Medical Center, Torrance, California 90502, USA

[5]Division of Cell Biology, Department of Pediatrics, National Jewish Health, Denver, Colorado 80206, USA

[6]Department of Developmental and Molecular Biology, Albert Einstein College of Medicine, Bronx, New York, USA

[7]Department of Internal Medicine II, Excellence Cluster Cardio-Pulmonary System, University of Giessen Lung Center, Klinikstrasse 36, Aulweg 130, 35392 Giessen, Germany

[#] These authors contributed equally to this work.

Abstract

Even though the role of the tyrosine phosphatase *Pten* as a tumor suppressor gene has been well established in thyroid cancer, its role during thyroid development is still elusive. We therefore targeted *Pten* deletion in the thyroid epithelium by crossing $Pten^{flox/flox}$ with a newly developed *Nkx2.1-cre* driver line in the BALB/c and C57BL/6 genetic backgrounds. C57BL/6 homozygous *Pten* mutant mice died around 2 weeks of age due to tracheal and esophageal compression by a hyperplasic thyroid. By contrast, BALB/c homozygous *Pten* mutant mice survived up to 2 years, but with a slightly increased thyroid volume. Characterization of the thyroid glands from C57BL/6 homozygous *Pten* mutant mice at postnatal day 14 (PN14) showed abnormally enlarged tissue with areas of cellular hyperplasia, disruption of the normal architecture, and follicular degeneration. In addition, differing degrees of hypothyroidism, thyroxine (T_4) decrease, and

(Correspondence should be addressed to P Minoo is now at General Lab Building, Women's and Children's Hospital, 1801 East Marengo Street, Los Angeles, California 90033, USA; minoo@usc.edu; S Belluci at Department of Internal Medicine II, Excellence Cluster Cardio-Pulmonary System, University of Giessen Lung Center; saverio.bellusci@innere.med.unigiessen.de).

Declaration of interest

The authors declare that there is no conflict of interest that could be perceived as prejudicing the impartiality of the research reported.

thyroid-stimulating hormone elevation between the strains in the mutants and the heterozygous mutant were detected at PN14. Finally, C57BL/6 heterozygous *Pten* mutant mice developed thyroid tumors after 2 years of age. Our results indicate that *Pten* has a pivotal role in thyroid development and its deletion results in thyroid tumor formation, with the timing and severity of the tumor depending on the particular genetic background.

Introduction

Thyroid tumors are one of the most common endocrine malignancies. Thyroid hyperplastic disorders can affect up to around 70% of the American population and can be present in a wide range of forms, from asymptomatic nodules detected by ultrasound to nodular hyperplasia (also called goiter) and neoplastic transformation (Ezzat *et al.* 1994, Rivas & Santisteban 2003). Recently, information on the molecular events controlling thyroid tumorigenesis has grown considerably. However, the exact molecular basis for this disease remains unclear.

Thyroid cells turn over very slowly as they divide only five times over the course of one's lifetime (Dumont *et al.* 1992), but the factors that limit the number of thyroid cells are not understood. Most thyrocytes appear capable of undergoing cell proliferation *in vivo* and *in vitro*, and the existence of stem cells that are able to replenish the pool offully differentiated thyrocytes has been postulated (Dumont *et al.* 1992).

Follicle homeostasis is thought to be maintained by a distinct pool of stem cells present in the adult thyroid gland. At least two types of thyroid stem cells have been described in the literature: the progenitor of follicular cells and the progenitor of C cells (Zhang *et al.* 2006). These stem cells could be the target of genetic alterations, giving rise to different forms of thyroid tumors. In the follicular cell lineage, papillary, follicular, hurtle, and anaplastic carcinomas have been detected, whereas medullary carcinomas are thought to be derived from C cells.

Loss of specific markers, such as calcitonin or thyroglobulin, is a common occurrence in several thyroid cancers. In these tumors, it is possible to recognize cancer cells with varying degrees of differentiation suggesting anomalous differentiation and maturation arrest of thyroid stem cells (Zhang *et al.* 2006).

Deregulation of PI3K signaling cascade through activation of PI3K and Akt and loss of *Pten* expression is frequently found in thyroid cancer (Coulonval *et al.* 2000). In addition, mutations in the *Pten* gene, encoding the major negative regulator of PI3K signaling, have been identified in Cowden's disease (CD; Scala *et al.* 1998), an autosomal dominant inherited cancer syndrome characterized by hamartomas of the skin, intestine, breast, and thyroid, as well as increased risk of developing breast and thyroid tumors (Eng 1998). Benign and malignant thyroid abnormalities occur in almost 70% of CD patients. Benign lesions in CD individuals include hyperproliferative diseases such as thyroiditis, multinodular goiters, and follicular adenomas. Presence of malignant epithelial thyroid tumors, which are primarily of follicular histotype, is observed in almost 10% of CD patients (Longy & Lacombe 1996). Recent reports have provided *in vivo* evidence of the

central role of the PI3K signaling cascade in controlling thyroid function and growth (Yeager *et al.* 2007, Antico-Arciuch *et al.* 2010). Deletion of the *Pten* gene in the thyroid follicular cells via the human thyroid peroxidase (TPO) gene promoter-cre system results in a phenotype resembling the features of CD and sporadic nontoxic goiter, which then progresses to follicular carcinomas.

In this study, we used a new model of thyroid-specific cre system, in which cre recombinase expression is under the control of the *Nkx2.1* promoter. *Nkx2.1* encodes a key regulator of thyroid, lung, and brain morphogenesis, whose onset of expression in mouse occurs around E9, at the beginning of thyroid morphogenesis. The murine *Nkx2.1* gene consists of three exons and a complex cis-active DNA region that controls its expression in the lung, brain, and thyroid (Pan *et al.* 2004). Our data show that *Pten* deletion in early embryonic stages is responsible for the development after birth of thyroid goiter and tumors in a strain-dependent manner. The current results validate and extend previous studies on the role of *Pten* in thyroid morphogenesis and provide a new direction in research on the physiology, regeneration, and carcinogenesis of the thyroid.

Materials and methods

Generation of *Nkx2.1-cre mouse*

Generation of *Nkx2.1-cre* transgenic line has been described (Xu *et al.* 2008). The *Nkx2.1-cre* transgenic mice were fertile and showed no obvious abnormalities.

Generation of $Pten^{Nkx2.1\text{-}cre}$ mice

C57BL/6 is a strain of wild-type mice with black coat color. BALB/c mice are albino. These sub-strains are among the inbred strains most widely used in animal experimentation.

$Pten^{flox/flox}$ females (BALB/c background and C57BL/6 background) were mated with *Nkx2.1-cre* male mice (C57BL/6 background; Tiozzo *et al.* 2009). The mice were backcrossed for five generations to obtain mice carrying *Nkx2.1-cre*; $Pten^{flox/flox}$ (herein referred to as $Pten^{Nkx2.1\text{-}cre}$ or homozygous mutants) and *Nkx2.1-cre*; $Pten^{flox/+}$ (hereafter referred to $Pten^{flox/+;Nkx2.1\text{-}cre}$ or heterozygous mutant) in an almost pure (>97%) BALB/c or C57BL/6 background. $Pten^{flox/flox}$ mice were used as control.

Genotyping of the *Nkx2.1-cre* mice (Xu *et al.* 2008) containing either $Pten^{flox}$ and $Pten^{wt}$ alleles was carried out as previously described (Lesche *et al.* 2002). All animal experiments were approved by the University of Southern California (USC) Animal Use and Care Committee.

Tissue collection

Embryonic thyroids from control and mutant embryos were collected at E13.5, E15.5, and E18.5. Adult mice (three $Pten^{Nkx2.1\text{-}cre}$ and three $Pten^{flox/flox}$ for each time point) were killed by CO_2 administration at 14 and 60 days. Heterozygous animals from two different backgrounds (BALB/c and C57BL/6) were killed at 2 yearsofage.Thethyroidsweredissected, fixed overnight, dehydrated through an increasing ethanol concentration gradient, and embedded in paraffin. Sections (5 mm) were mounted on slides for histological analysis.

Immunohistochemistry analysis

Sections were deparaffinized with two changes of xylene and hydrated with a successive ethanol concentration gradient. Immunohistochemistry (IHC) of the tissue samples for NKX2.1, *Pten*, and P-AKT was performed using antigen retrieval, in which the samples were boiled for 20 min in Na-citrate buffer (10 mM, pH 6.0) and incubated with Ab-NKX2.1 (1:1500, Seven Hills, Cincinnati, OH, USA), Ab-*Pten* (1:100, Cell Signaling, Danvers, MA, USA), and Ab-P-AKT (1:50, Cell Signaling). The signal was visualized with the Histostain Rabbit Primary Kit (Zymed–Invitrogen), as instructed by the manufacturer. Antibody incubation for E-cadherin (1:200, BD) and phosphohistone H3 (PH3) (1:200, Cell Signaling) was performed in tris-buffered saline (TBS), with 3% BSA and 0.1% Triton X-100 overnight at 4 °C. The secondary antibodies were obtained from Jackson Immunoresearch (West Grove, PA, USA) and Vecta-shield. Photomicrographs were taken using a Leica DMRA fluorescence microscope with a Hamamatsu Digital Camera CCD and Zeiss Axioplan (Germany).

Cell proliferation analysis

Cell proliferation was assessed using PH3 and E-cadherin staining on E15.5- and P14-day-old thyroids. After antigen retrieval (see above), the sections were incubated overnight at 4 °C with Ab-PH3 (1:200, Cell Signaling) and Ab-E-cadherin (1:200, BD). Signals were visualized by following the manufacturer's instructions. Finally, the slides were counterstained with 4′,6-diamidino-2-phenylindole (DAPI). The total number of E-cadherin positive cells and the number of PH3/E-cadherin positive cells in the thyroid's epithelium were scored using ten photomicrographs (40× magnification) taken at random locations within sections of a given mutant thyroid (three independent mutants were used for this analysis). The same procedure was repeated for sections from three control thyroids. An ANOVA test evaluated the significance of the difference in proliferation between the control and mutant thyroids.

LacZ staining

Thyroids at different developmental stages were dissected and fixed in 4% paraformaldehyde for 10 min, washed twice for 10 min in PBS, transferred to freshly prepared X-gal solution, and stained at 37 °C until a clear precipitate formed. After rinsing with PBS, the tissues were post-fixed in 4% paraformaldehyde in PBS. For vibratome sections, samples were embedded in an albumin (300 mg/ml)–gelatin (5 mg/ml) mix, cross-linked with glutaraldehyde (0.6%), and sectioned at 30 μm. For microtome sections, thyroids were fixed in 4% paraformaldehyde, washed in PBS, dehydrated, and embedded with paraffin. Sections were counter-stained with eosin for 5 min.

RNA extraction and quantitative RT-PCR

Total RNA was isolated from thyroids of transgenic mice and wild-type littermate controls using a Qiagen RNAeasy kit by following its manufacturer's specifications. A Nano Drop ND-1000 was used to determine the concentration of the purified RNA.

Total RNA (5 μg) was reverse-transcribed using the Superscript-III first strand super mix (Invitrogen), in accordance with the manufacturer's directions. Twenty-five picograms of

cDNA was used for each of the real-time PCR reactions using the primers and probes designed by the online Roche Software: probe finder version 2.20, https://www.roche-applied%1Escience.com/sis/rtpcr/upl/adc.jsp.

The following primers were used:

OCT4: left, gttggagaaggtggaaccaa; right, ctccttctgcagggctttc, probe 95.

SCA1: left, cccctaccctgatggagtct; right, tgttctttactttccttgtttgagaa, probe 16.

P63: left, agacctcagtgaccccatgt; right, ctgctggtccatgctgttc, probe 45.

PTEN: left, aggcacaagaggccctagat; right, ctgactgggaattgtgactcc, probe 60.

Pax8: left, gcagctatgcctcttctgcta; right, gctgtaggcattgccagaat, probe 4.

TTF1: left, catgccttcagactgcacat; right, tctttgcacggtagtacacga, probe 81.

TTF2: left, aaccccaaacagagaatgga; right, caagagggagatcagcatgac, probe 22.

Beta-actin: left, tgacaggatgcagaaggaga; right, cgctcaggaggagcaatg, probe 106.

All real-time PCR reactions were performed with Roche FastStart TaqMan Probe Master kits according to the manufacturer's instructions in a Roche Light Cycler 1.5 Real-Time PCR machine. Beta-actin RNA was used as an internal control for all analyses.

Hormone measurements

Blood was collected by retro-orbital puncture, and serum was stored at −80 °C until analysis. Total thyroxine (T_4) and thyroid-stimulating hormone (TSH) were measured by RIA at the Harbor-University of California at Los Angeles Medical Center (Torrance, CA, USA).

Data presentation and statistical analysis

Data were presented as mean ± S.E.M., unless stated otherwise. Statistical analysis was carried out using an ANOVA test so as to compare the two groups. P values ≤0.05 were considered significant.

Results

Nkx2.1-cre recombinase driver mouse line

The pattern and efficiency of the *Nkx2.1-cre* line in mediating LoxP-dependent excision in the thyroid epithelium was determined using *Rosa26R-lacZ* reporter mice. LacZ activity was virtually absent in the wild-type thyroids (data not shown), whereas in E9 *Rosa26R-lacZ*$^{Nkx2.1\text{-}cre}$ thyroids, LacZ activity was limited to the primordial lung, thyroid, and brain (Fig. 1A and B). At E13.5, it was possible to detect LacZ activity in the thyroid and tracheal epithelium (Fig. 1C and D) of the *Rosa26R-lacZ*$^{Nkx2.1\text{-}cre}$ embryos. It is to be noted that as expected, LacZ activity was absent in the parathyroids (Fig. 1D). In postnatal day 15 (PN15) thyroid, the pattern of LacZ activity was homogeneous in all the epithelial cells (Fig. 1E and F). Thus, *Nkx2.1-cre* mice represent a novel and useful tool for conditional deletion of epithelial genes during early thyroid development.

Thyroid epithelial-specific deletion of *Pten* by *Nkx2.1-cre*

To determine the potential role of *Pten* in thyroid morphogenesis, *Pten* was deleted in the thyroid epithelium using the *Nkx2.1-cre* mouse line. Homozygous deletion of *Pten* via *Nkx2.1-cre* resulted in postnatally viable mice with a frequency consistent with the expected Mendelian ratio. IHC in $Pten^{Nkx2.1\text{-}cre}$ thyroids at E18.5 showed that the PTEN protein was absent in 100% of the epithelial cells, whereas positive staining was detected in the mesenchymal cells (Fig. 2D and D′). PTEN-negative epithelial cells in the mutant thyroids were positive for *Nkx2.1*, indicating their epithelial cell identity (Fig. 2B and B′), and showed an increase of phospho-Akt staining (compare Fig. 2F and F′ with Fig. 2E and E′), demonstrating the activation of the PI3K pathway. *Pten* deletion was confirmed by qPCR, using RNA from P14 mutant and control thyroid tissue (in both BALB/c and C57BL/6 backgrounds). This analysis showed a statistically significant decrease of *Pten* transcripts in the mutants compared with the control, confirming *Pten* deletion (Fig. 2G: C57BL/6 background/mean normalized ratio 0.14±0.07, BALB/c background/mean normalized ratio 0.10±0.05, *$p<0.05$). At E15.5, comparison between the C57BL/6 homozygous mutants and the controls showed that although there was a significant increase in mutant thyroids' size, morphologically the thyroids appeared identical (Fig. 3A and B). At PN14, thyroid enlargement in the homozygous mutant mice in C57BL/6 background compared with the controls was striking (Fig. 3C and D, G and H: statistical analysis of the thyroid weight: control 1.1±0.09 mg vs mutants 11.1±1 mg, $n=10$ for each group). Moreover, the thyroid architecture was altered, with multilayered epithelial cells surrounding the colloid lumen and with some dysmorphic follicles that contained abnormal material inside (Fig. 3E and F).

Quantification of the number of E-cadherin (marker for epithelial cells) and phosphohistone 3 (marker for proliferation) double-positive cells at E15.5 (Fig. 4A–C) and PN14 (Fig. 4D–I) showed an increase in epithelial cell proliferation rate in the mutants compared with the controls at E15.5 (control 0.1 ±0.0% vs mutant 6.2G±0.9%, $P<0.01$) and at PN14 (C57BL/6 background: control 0.1±0.07% vs mutant 0.9±0.15%, $P<0.01$; BALB/c background: control 0.06±0.04% vs mutant 0.2±0.09%, $P<0.05$; $n=5$ for each group; Fig. 4C, F and I).

Of note, at PN14, the differences between the mutant and control proliferation rates were higher in the C57BL/6 background compared with the BALB/c background (Fig. 4F–I).

These results indicate that in our mouse model, early epithelial deletion of *Pten* in the thyroid causes epithelial hyperplasia and follicle dysmorphism, which are detectable from early development to adult and are due to increased epithelial cell proliferation.

Early *Pten* deletion leads to a range of phenotypic severity based on the genetic background

Different thyroid phenotypes were observed depending on the genetic background. At PN14, in the BALB/c strain, the architecture was conserved and it was possible to observe only an increased number of epithelial cells along the follicles (Fig. 5A and B), resembling a goiter disease. In the C57BL/6 background, on the other hand, the thyroid structure was completely altered with multiple small degenerative follicles, which had varying degrees of colloid depletion (Fig. 5C), resembling a follicular adenoma. Although the mutants for both

lines of mice had an enlarged thyroid, the genetic background of the animals determined their overall outcome. In the BALB/c background, the homozygous mice survived to adulthood without presenting with any obvious pathological conditions, whereas in the C57BL/6 strain all the homozygous animals died before 2 weeks of age due to compression of the trachea and esophagus by the enlarged thyroid.

We found a statistically significant decrease in T_4 hormonal levels (Fig. 5G) and increase of TSH in the PN14 C57BL/6 homozygous mutants compared with controls (T_4: 2.69±0.85 vs 6.47±0.14, $P<0.05$, $n=5$; TSH: 7.1±0.8 vs 2.8±0.8, $P<0.05$, $n=5$). In the corresponding BALB/c background, such differences were not found (Fig. 5G; T_4: 4.1±0.6 vs 4.5±0.3, P = not significant (NS), $n=5$; TSH: 3.65±0.9 vs 5.1±0.9, P=NS, $n=5$).

Hormone measurements were also carried out in PN14 heterozygous mutant mice for each genetic background ($n=5$ per genetic background). C57BL/6 heterozygous mutant mice showed a mild decrease of T_4 but no significant increase of TSH compared with the corresponding hormone levels in the controls (T_4: 4.8±0.14 vs 6.47±0.14, $P<0.05$; TSH: 3±0.01 vs 2.8±0.8, $P>0.05$). BALB/c heterozygous mutants, on the other hand, showed a statistically significant increase in the level of T_4 that did not correlate with a change in the level of TSH (T_4: 6.3±0.3 vs 4.1±0.6, $P<0.05$; TSH: 4.5±1.25 vs 5.1±0.9, $P>0.05$).

Additionally, 100% of the *Pten*$^{flox/C;Nkx2.1\text{-}cre}$ heterozygous animals in the C57BL/6 background developed thyroid tumors after ~2 years of age (Fig. 5F), whereas the thyroids of the corresponding BALB/c heterozygous mice were only enlarged (Fig. 5E). To determine the nature of the tumors, we performed histological analyses on the thyroids from controls and heterozygous *Pten*$^{flox/C;Nkx2.1\text{-}cre}$ 2-year-old mice in the C57BL/6 and BALB/c backgrounds. Control thyroids exhibited normal histology with structured colloid-filled follicles (Fig. 6A and D). BALB/c heterozygous *Pten*$^{flox/C;Nkx2.1\text{-}cre}$ thyroids showed enlarged follicles (Fig. 6B and E). However, C57BL/6 heterozygous *Pten*$^{flox/C;Nkx2.1\text{-}cre}$ animals showed an altered thyroid structure with normal areas that included not only colloid-filled follicles but also abnormal areas with focal hyperplasia, polynuclear cells, small nonencapsulated areas of hypercellularity with solid and/or microfollicular patterns and internal hemorrhage (Fig. 6C and F). These results showed that *Pten* gene dosage reduction in the thyroid epithelium leads to differentiated follicular tumors only in a specific background (C57BL/6), whereas a similar decrease in *Pten* expression in BALB/c heterozygous mice leads to a goiter-like phenotype.

Pten deletion impacts thyroid epithelial cell differentiation and increases the progenitor cell pool in the thyroid

To determine the impact of epithelial *Pten* deletion on thyroid differentiation and the differences between the phenotypes, the expression of different cell markers was examined by qPCR in PN14 thyroids from homozygous *Pten*$^{Nkx2.1\text{-}cre}$ and *Pten*$^{flox/flox}$ (control) mice in both backgrounds. Stem cell markers, such as *p63*, *Oct4*, and *Sca-1*, were decreased in the mutant in both C57BL/6 and BALB/c backgrounds (Fig. 6G; *p63* C57BL/6 background 0.655±0.2, BALB/c background 0.2± 0.0; *Oct4* C57BL/6 background 0.33±0.27, BALB/c background 0.02±0.01; *Sca-1* C57BL/6 background 0.21±0.2, BALB/c background 0.25±0.09), suggesting a decrease of the stem cell pool size in the mutant thyroids. Thyroid

transcriptional factors such as *Ttf1*, *Pax8*, and *Ttf2* were not significantly changed or increased (Fig. 6H; *Ttf1* C57BL/6 background 0.81± 0.17, *Ttf1* BALB/c background 0.56±0.15, *Ttf2* C57BL/6 background 1.79±0.3, *Ttf2* BALB/c background 0.73±0.3, *Pax8* C57BL/6 background 2.42± 1.3, *Pax8* BALB/c background 1.03±0.11). Most drastic variations occurred in the C57BL/6 background, whereas in the BALB/c background there was a minimal decrease or no changes.

These results indicate that *Pten* plays a necessary function in normal thyrocyte cell fate and in thyroid progenitor pool maintenance, depending on the genetic background.

Discussion

To date, the molecular mechanisms responsible for the ontogeny of thyroid tumors are not fully understood. Several studies and clinical data have connected the PI3K/Akt pathway with thyroid proliferative disorders. *Pten* mutations are recognized as being the cause of CD, a syndrome characterized by tumors in different tissues, including the thyroid (Nelen *et al.* 1997). Moreover, recent studies have shown that deletion of *Pten* in the thyroid leads to goiter and adenomas (Yeager *et al.* 2007) that then progress to tumors (Antico-Arciuch *et al.* 2010). In these studies, the authors deleted *Pten* in a 129Sv background using the *TPO-cre* driver line, whose expression starts at about E14.5. As a result, only cells already committed to thyroid differentiation were affected (Kusakabe *et al.* 2004). In our study, we used two different backgrounds, BALB/c and C57BL/6. In addition, we used a different driver line where *cre* expression is under the control of the *Nkx2.1* promoter, which starts being expressed in the foregut endoderm domain that will give rise to the lung and thyroid. As it is expressed early in development, *Nkx2.1-cre* activity had an impact on the primitive thyroid, where the cells start to commit to thyroid differentiation. Moreover, we were able to observe a different phenotype based on the different genetic backgrounds. The $Pten^{Nkx2.1\text{-}cre}$ homozygous mice in C57BL/6 background were not able to survive after the second week of life due to tracheal and esophageal compression from an enlarged thyroid. $Pten^{Nkx2.1\text{-}cre}$ homozygous mice in BALB/c background were able to survive, presenting a mild thyroid hyperplasia. In addition, the C57BL/6 heterozygous mutant mice showed a decrease of T_4 level, but were able to survive and developed follicular tumors over time. BALB/c homozygous and heterozygous mutant mice surpassed the 2 weeks lifespan of the homozygous mutant C57BL/6 mice and eventually showed a simple thyroid hyperplasia at about 2 years of age. One possible explanation for this different phenotype can be attributed to the different types of cells present in the two groups of mutants. Quantification of the markers for thyroid stem cells such as *Sca-1*, *p63*, and *Oct4* showed that in both genetic backgrounds, these cells were decreased in number in comparison with the control. However, *Ttf2* and *Pax8* were increased in the C57BL/6 background compared with the BALB/c background. Considering that *Ttf2* and *Pax8* are the transcription factors present at the onset of thyroid development, they can be considered as markers for progenitor cells already committed or transient amplifying cells. These results suggest that the oncogenic effect of *Pten* deletion in thyroid carcinogenesis can be due to an increase of transient amplifying cells positive for *Ttf2* and *Pax8*.

Another difference between the two studies is the genetic background of the mice. The Sv129Sv background used by Yeager *et al.* (2009) gave an intermediate phenotype, similar to our studies on BALB/c, resulting in goiter development with no significant changes in hormonal levels until later in life when we found increased T_4 (without suppression of TSH) and neoplastic transformation. However, the C57BL/6 background resulted in a phenotype showing diminished thyroid hormone levels in both mutants and heterozygous mice (with TSH elevation only in the mutant) and eventually developing thyroid tumors in the heterozygous mice over time. Critical future experiments will be levothyroxine ($_L$-T_4) treatment of the C57BL/6 heterozygous mice to determine whether some of the differences in the phenotype could be possibly related to the TSH increase. In fact, the difference in TSH levels can cause the difference in thyroid growth in the two backgrounds.

The proliferation rate was already altered during the embryonic stage at E15.5 (Fig. 4A–C). Examining the adults, it was possible to observe a larger difference between the control and the mutants in the C57BL/6 compared with the BALB/c backgrounds. This may potentially be one of the reasons for the significant phenotypic differences observed in the C57BL/6 background compared with the mild phenotype in BALB/c background. The differences in phenotype may simply be related to the different time points at which *cre* was activated in these two backgrounds or more generally to the different genetic backgrounds of the mice. The latter has been well documented by observations that link onset and severity of tumorigenesis to the genetic background of *Pten* knockout mice (Freeman *et al.* 2006).

Activation of Akt in thyroid tumors is well established (Ringel *et al.* 2001). In our mouse model, the increase of phospho-Akt was detected as early as at E15.5 in the mutant thyroids. However, more in-depth studies are necessary to determine whether this increase is the main reason for the increase in epithelial cell proliferation and the appearance of tumors. In fact, the increase in cell proliferation could be related not to a difference in thyroid cell sensitivity to *Pten* loss in the two strains, but simply to the differences in circulating TSH levels. Indeed, TSH is known to cooperate with PI3K signaling both *in vitro* and *in vivo* to dramatically enhance proliferative capacity of thyroid cells (Kimura *et al.* 2001). Interestingly, levels of TSH were normal in C57BL/6 heterozygous mutant compared with control mice (Fig. 5G) in spite of the fact that these mice developed thyroid cancer later at 2 years of age. Even though we cannot exclude that TSH could be progressively increased in these mice as they age, our data suggest that in addition to a potential effect of elevated TSH on the proliferation of the epithelial progenitors, epithelial deletion of *Pten* in the thyroid also has a cell-autonomous effect, which is at least partially responsible for the amplification of the thyroid epithelial progenitors. For a reason that still remains to be indentified, this effect seems to be increased in the C57BL/6 backgroundvs the BALB/c background. Such a cell-autonomous (non-hormone dependent) effect of *Pten* deletion was also observed in our previous work on the role of *Pten* in the lung (Tiozzo *et al.* 2009).

Several studies report that loss of thyroid-specific proteins and the presence of cells with different degrees of differentiation is a common feature in thyroid carcino-genesis (Brabant *et al.* 1991, Lazar *et al.* 1999). These anomalies can suggest a situation of abnormal differentiation and maturation arrest as basic traits of the thyroid cancer stem cells. In human tumors, the overexpression of *Ttf1* and *Pax8* may induce the differentiation of anaplastic

thyroid carcinoma (van der Kallen *et al.* 1996, Mansouri *et al.* 1998),whereas the underexpression of *Ttf1* and *Pax8* correlates with the aggressiveness of thyroid carcinomas. In our work, *Ttf1* and *Pax8* were not altogether missing, which may explain the slow growth of the tumor.

In conclusion, our data show that activation of the PI3K/Akt pathway results in two different phenotypes depending on the genetic background of the mutant mice. Both goiter and adenomas in the BALB/c background and follicular thyroid tumors in C57BL/6 background are features of CD. Secondly, the presence of more committed progenitor cells in the C57BL/6 mice compared with BALB/c suggests that this may be linked to the different outcome of hyperplasia and tumor development in C57BL/6 mice.

Acknowledgments

Funding

This work was supported by NIH PO1 HL060231 (P Minoo), R01HL086322 and the Excellence Cluster in Cardio-Pulmonary System (S Bellusci), R01HL092967 (S De Langhe), and R01 CA128943 (A Di Cristofano); Hastings Foundation (P Minoo); CIRM Clinical Fellowship (C Tiozzo); and 'Young Investigator Award', European Society of Pediatrics (C Tiozzo).

References

Antico-Arciuch VG, Dima M, Liao XH, Refetoff S, Di Cristofano A. Cross-talk between PI3K and estrogen in the mouse thyroid predisposes to the development of follicular carcinomas with a higher incidence in females. Oncogene. 2010; 29:5678–5686. (doi:10. 1038/onc.2010.308). [PubMed: 20676139]

Brabant G, Maenhaut C, Köhrle J, Scheumann G, Dralle H, Hoang-Vu C, Hesch RD, von zur Mühlen A, Vassart G, Dumont JE. Human thyrotropin receptor gene: expression in thyroid tumors and correlation to markers of thyroid differentiation and dedifferentiation. Molecular and Cellular Endocrinology. 1991; 82:R7–12. (doi:10.1016/ 0303-7207(91)90018-N). [PubMed: 1761161]

Coulonval K, Vandeput F, Stein RC, Kozma SC, Lamy F, Dumont JE. Phosphatidylinositol 3-kinase, protein kinase B and ribosomal S6 kinases in the stimulation of thyroid epithelial cell proliferation by cAMP and growth factors in the presence of insulin. Biochemical Journal. 2000; 348(Pt 2):351–358. doi:10.1042/0264-6021:3480351. [PubMed: 10816429]

Dumont JE, Lamy F, Roger P, Maenhaut C. Physiological and pathological regulation of thyroid cell proliferation and differentiation by thyrotropin and other factors. Physiological Reviews. 1992; 72:667–697. [PubMed: 1320763]

Eng C. Genetics of Cowden syndrome: through the looking glass of oncology. International Journal of Oncology. 1998; 12:701–710. [PubMed: 9472113]

Ezzat S, Sarti DA, Cain DR, Braunstein GD. Thyroid incidentalomas. Prevalence by palpation and ultrasonography. Archives of Internal Medicine. 1994; 154:1838–1840. (doi:10.1001/archinte. 1994.00420160075010).

Freeman D, Lesche R, Kertesz N, Wang S, Li G, Gao J, Groszer M, Martinez-Diaz H, Rozengurt N, Thomas G, et al. Genetic background controls tumor development in PTEN-deficient mice. Cancer Research. 2006; 66:6492–6496. (doi:10.1158/0008-5472.CAN-05-4143). [PubMed: 16818619]

van der Kallen CJ, Spierings DC, Thijssen JH, Blankenstein MA, de Bruin TW. Disrupted co-ordination of Pax-8 and thyroid transcription factor-1 gene expression in a dedifferentiated rat thyroid tumour cell line derived from FRTL-5. Journal of Endocrinology. 1996; 150:377–382. (doi: 10. 1677/joe.0.1500377). [PubMed: 8882156]

Kimura T, Van Keymeulen A, Golstein J, Fusco A, Dumont JE, Roger PP. Regulation of thyroid cell proliferation by TSH and other factors: a critical evaluation of in vitro models. Endocrine Reviews. 2001; 22:631–656. (doi:10.1210/er.22.5.631). [PubMed: 11588145]

Kusakabe T, Kawaguchi A, Kawaguchi R, Feigenbaum L, Kimura S. Thyrocyte-specific expression of cre recombinase in transgenic mice. Genesis. 2004; 39:212–216. (doi:10.1002/gene.20043). [PubMed: 15282748]

Lazar V, Bidart JM, Caillou B, Mahé C, Lacroix L, Filetti S, Schlumberger M. Expression of the Na^C/I^K symporter gene in human thyroid tumors: a comparison study with other thyroid-specific genes. Journal of Clinical Endocrinology and Metabolism. 1999; 84:3228–3234. (doi:10.1210/jc.84.9.3228). [PubMed: 10487692]

Lesche R, Groszer M, Gao J, Wang Y, Messing A, Sun H, Liu X, Wu H. Cre/loxP-mediated inactivation of the murine Pten tumor suppressor gene. Genesis. 2002; 32:148–149. (doi:10.1002/gene.10036). [PubMed: 11857804]

Longy M, Lacombe D. Cowden disease. Report of a family and review. Annales de Génétique. 1996; 39:35–42. [PubMed: 9297442]

Mansouri A, Chowdhury K, Gruss P. Follicular cells of the thyroid gland require Pax8 gene function. Nature Genetics. 1998; 19:87–90. (doi:10.1038/ng0598-87). [PubMed: 9590297]

Nelen MR, van Staveren WC, Peeters EA, Hassel MB, Gorlin RJ, Hamm H, Lindboe CF, Fryns JP, Sijmons RH, Woods DG, et al. Germline mutations in the PTEN/MMAC1 gene in patients with Cowden disease. Human Molecular Genetics. 1997; 6:1383–1387. (doi:10.1093/hmg/6.8.1383). [PubMed: 9259288]

Pan Q, Li C, Xiao J, Kimura S, Rubenstein J, Puelles L, Minoo P. In vivo characterization of the Nkx2.1 promoter/enhancer elements in transgenic mice. Gene. 2004; 331:73–82. (doi:10.1016/j.gene.2004.01.026). [PubMed: 15094193]

Ringel MD, Hayre N, Saito J, Saunier B, Schuppert F, Burch H, Bernet V, Burman KD, Kohn LD, Saji M. Overexpression and overactivation of Akt in thyroid carcinoma. Cancer Research. 2001; 61:6105–6111. [PubMed: 11507060]

Rivas M, Santisteban P. TSH-activated signaling pathways in thyroid tumorigenesis. Molecular and Cellular Endocrinology. 2003; 213:31–45. (doi:10.1016/j.mce. 2003.10.029). [PubMed: 15062572]

Scala S, Bruni P, Lo Muzio L, Mignogna M, Viglietto G, Fusco A. Novel mutation of the PTEN gene in an Italian Cowden's disease kindred. International Journal of Oncology. 1998; 13:665–668. [PubMed: 9735393]

Tiozzo C, De Langhe S, Yu M, Londhe VA, Carraro G, Li M, Li C, Xing Y, Anderson S, Borok Z, et al. Deletion of Pten expands lung epithelial progenitor pools and confers resistance to airway injury. American Journal of Respiratory and Critical Care Medicine. 2009; 180:701–712. (doi:10.1164/rccm.200901-0100OC). [PubMed: 19574443]

Xu Q, Tam M, Anderson SA. Fate mapping Nkx2.1-lineage cells in the mouse telencephalon. Journal of Comparative Neurology. 2008; 506:16–29. (doi:10.1002/cne.21529). [PubMed: 17990269]

Yeager N, Klein-Szanto A, Kimura S, Di Cristofano A. Pten loss in the mouse thyroid causes goiter and follicular adenomas: insights into thyroid function and Cowden disease pathogenesis. Cancer Research. 2007; 67:959–966. (doi:10.1158/0008-5472.CAN-06-3524). [PubMed: 17283127]

Zhang P, Zuo H, Ozaki T, Nakagomi N, Kakudo K. Cancer stem cell hypothesis in thyroid cancer. Pathology International. 2006; 56:485–489. (doi:10.1111/j.1440-1827.2006.01995.x). [PubMed: 16930327]

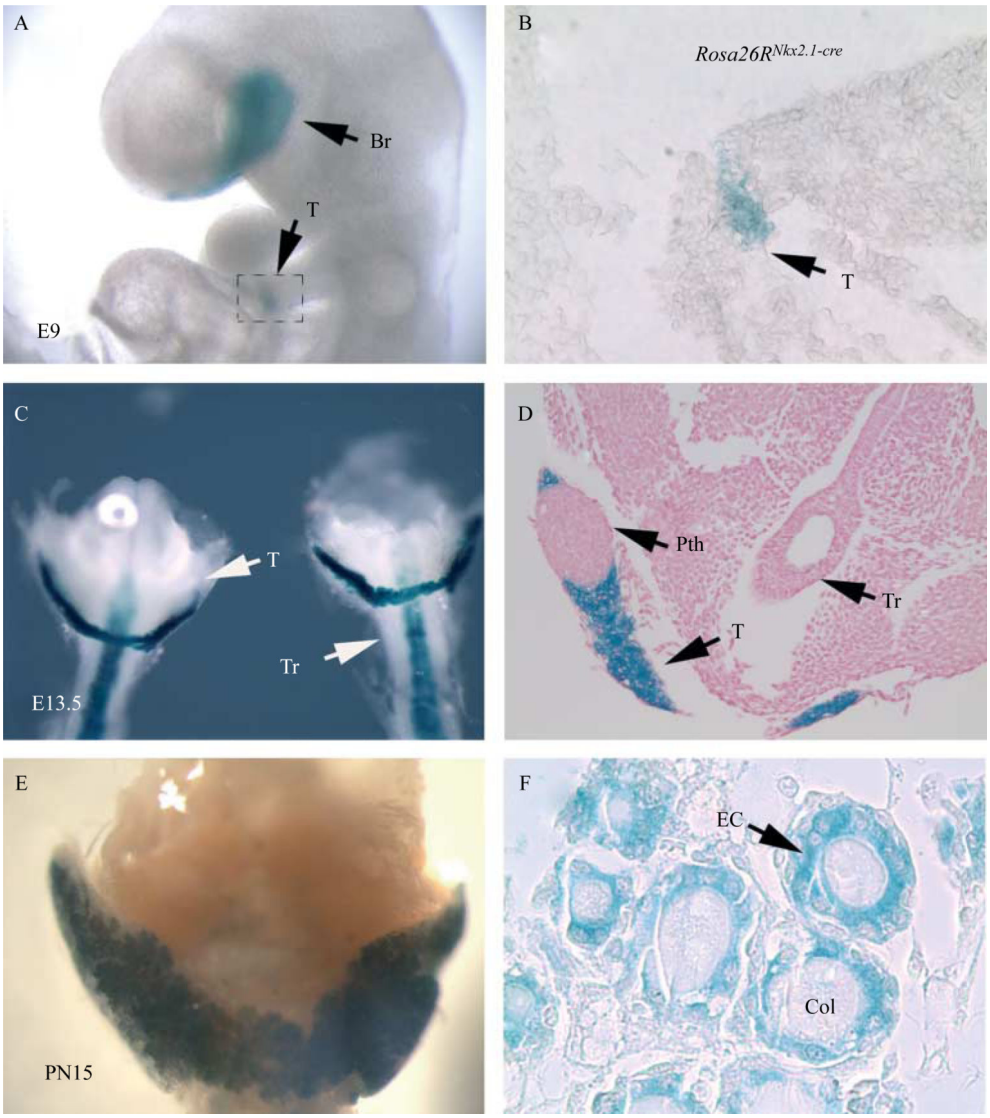

Figure 1.

LacZ staining of *Rosa26R*$^{Nkx2.1\text{-}cre}$ (A and B) E9 embryos, and thyroids at (C and D) E13.5 and (E and F) PN15, showing *cre* specific activity in the epithelial cells in the thyroid. (D) As expected, the cells in the parathyroids are negative for LacZ staining. Br, brain; T, thyroid; Pth, parathyroids; EC, epithelial cells; Col, colloids.

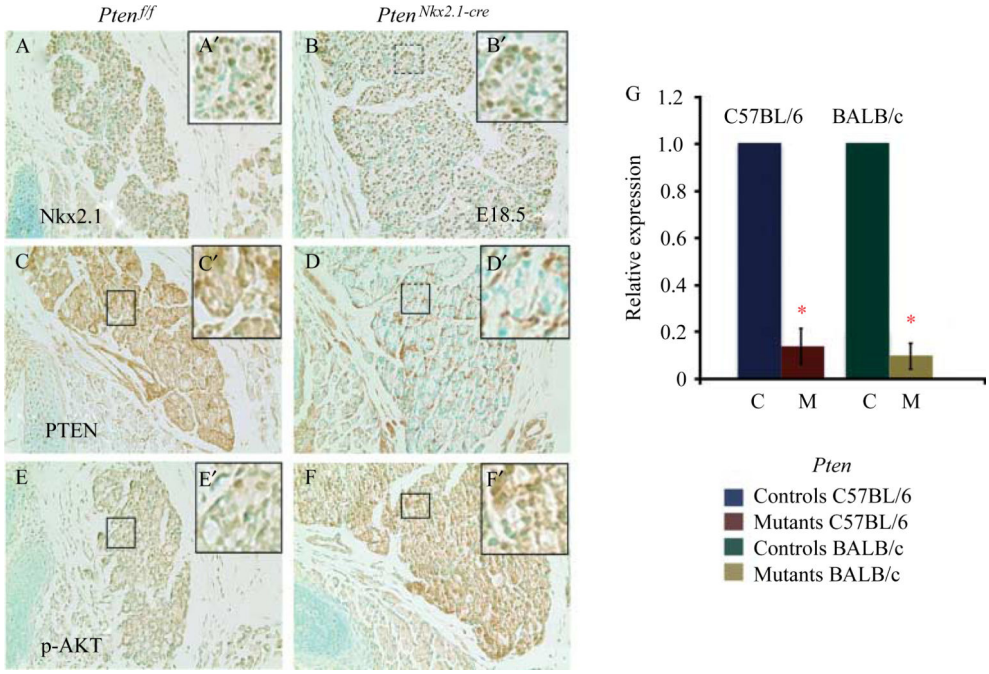

Figure 2.

E18.5 (A, C, and E) control and (B, D, and F) mutant thyroids stained for (A and B) NKX2.1, (C and D) PTEN, and (E and F) p-AKT. Note that the *Nkx2.1*-positive cells are detected in the mutant. *Pten* expression is strongly decreased in the mutant epithelial cells. Conversely, p-AKT signal is increased in the mutant thyroid. Upper right panels are the corresponding high magnification pictures. (G) Relative expression level for *Pten* by qPCR proving *Pten* deletion in the mutant thyroids in both C57BL/6 and BALB/c genetic backgrounds. *$p<0.05$.

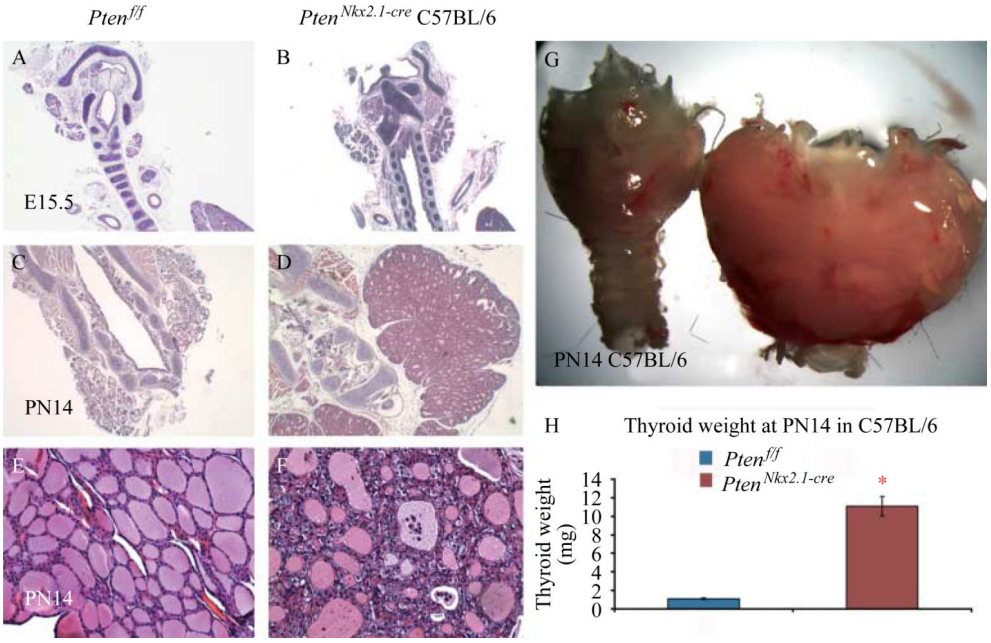

Figure 3.

H and E staining of (A, C, and E) control and (B, D, and F) C57BL/6 homozygous mutant thyroids at different stages, demonstrating that in *Pten* mutants, the increase in size starts very early during thyroid organogenesis (compare B with A at E15.5). (C–G) At the adult stage, mutant thyroids are enlarged, with multilayered epithelial cells surrounding the colloid lumen. Some follicles are dysmorphic with abnormal material inside. (H) Statistical analysis of the weight of *P*=14 thyroids (*n*=10 for mutant and wild-type). $p<0.05$.

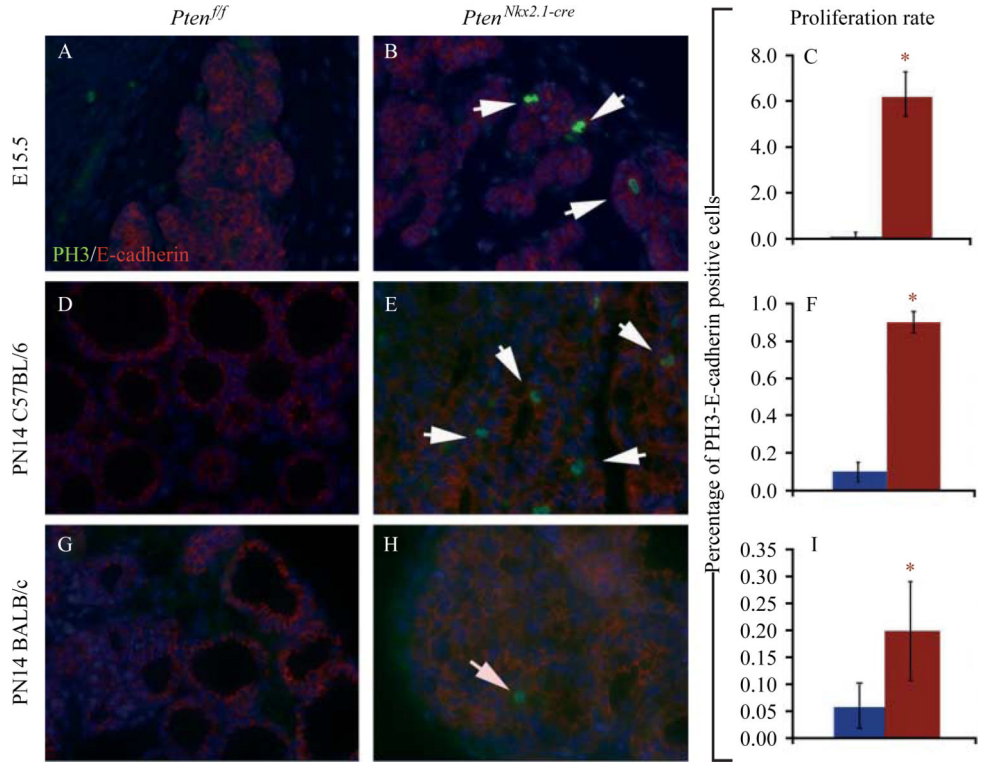

Figure 4.

Double IF staining for PH3 (marker for proliferation) and E-cadherin (marker for epithelial cells) as well as quantification of the number of E-cadherin and phosphohistone H3 double-positive cells in control and mutant thyroids at (A–C) E15.5 and (D–F, C57BL/6 background; G–I, BALB/c background) PN14 (n=3 for each group). Note that in the BALB/c background, the increase in epithelial proliferation is not as pronounced compared with the one observed in the C57BL/6 background. Note that for proliferation at E15.5, no differences were observed between both genetic backgrounds. White arrows in B, E and H indicate double positive cells for E-cadherin and phosphohistone H3. p<0.05.

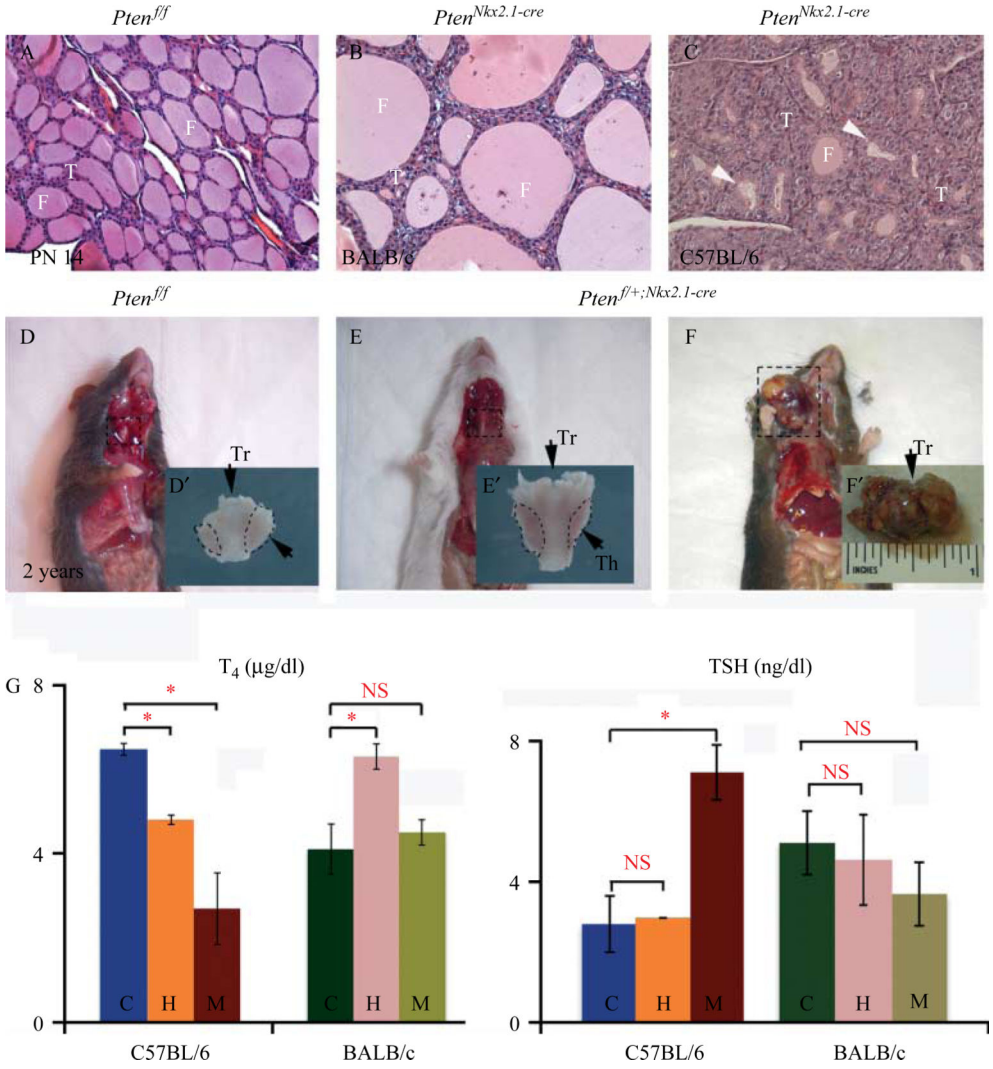

Figure 5.

Phenotypic differences between the two genetic backgrounds. H and E staining of (A) control, (B) homozygous mutant BALB/c, and (C) homozygous mutant C57BL/6. Note that in the C57BL/6 background, the phenotype is more severe with dysmorphic and involuted follicles (panel C white arrow), while in the BALB/c background, the follicles appear only enlarged (B) compared with the control. (D) Two-year-old mice control, (E) heterozygous BALB/c, and (F) heterozygous C57BL/6. The C57BL/6 heterozygous mice develop tumors at the thyroid level, while the BALB/c heterozygous mice present only with hypertrophic thyroid. (G) T_4 and TSH hormone levels at PN14. In the C57BL/6 background, we observe a statistically significant decrease in T_4 in both mutants and heterozygous animal, but a statistically significant increased level of TSH compared with the control was observed only in the mutant. In the BALB/c background, on the other hand, homozygous and heterozygous mutant levels are similar to the controls for TSH (n=5 for each group). Th, thyroid; Tr, trachea.

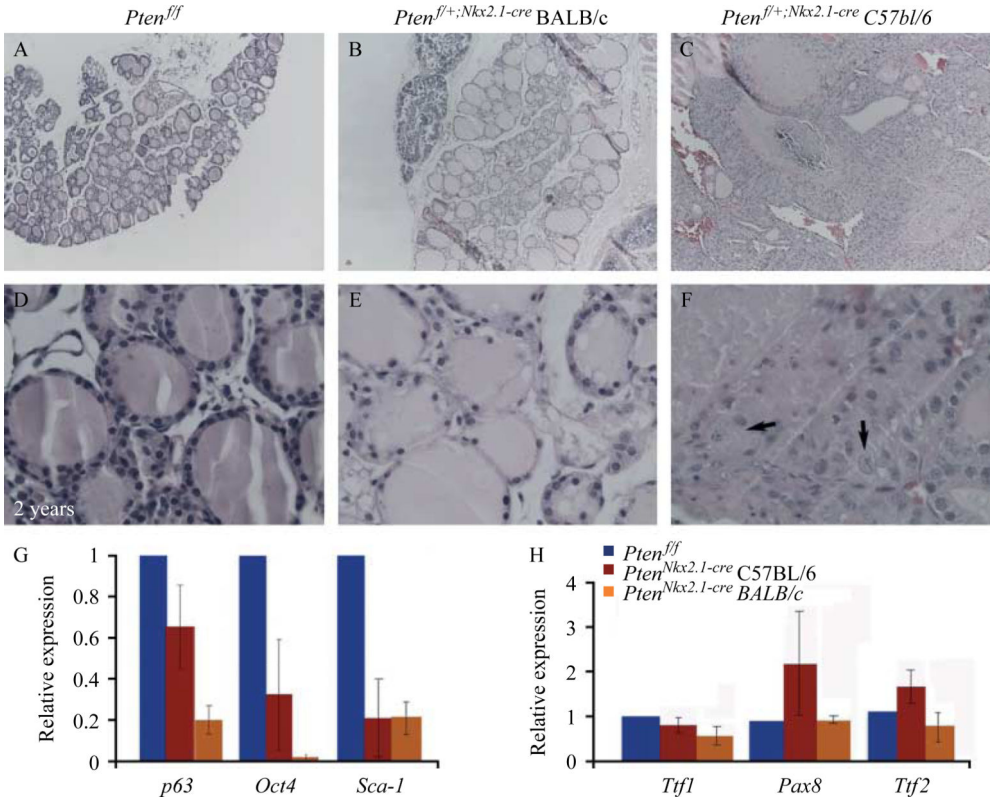

Figure 6.

Hematoxylin and eosin staining of (A) control and (B and C) heterozygous thyroids at 2 years of age. (A) Control thyroids show normal histology with structured colloid-filled follicles. (B) Heterozygous *Pten*$^{flox/C;Nkx2.1\text{-}cre}$ BALB/c thyroids show enlarged follicles in the middle of areas of atrophy. (C) Heterozygous *Pten*$^{flox/C;Nkx2.1\text{-}cre}$ thyroids in C57BL/6 background display thyroid structure that was altered, with normal areas presenting not only with colloid-filled follicles but also with focal hyperplasia, small nonencapsulated areas of hypercellularity with solid and/or microfollicular patterns. (D–F) Corresponding high magnification pictures. Arrows in (F) indicate cells with more than one nucleus. (G and H) Real-time PCR analysis of key stem cell genes. (G) Expression levels of *p63*, *Oct4*, and *Sca-1* showing the decrease of all stem cell markers in both C57BL/6 and BALB/c homozygous mutants compared with control thyroids. (H) Thyroids in the C57BL/6 background display increased expression of the transcriptional factors *Pax8* and *Ttf2*. Such an increase was not detected in the BALB/c homozygous mutant thyroids.